

# Deep lenses of circumpolar water in the Argentine Basin

M. Arhan and X. Carton

Laboratoire de Physique des Océans, CNRS/IFREMER/UBO, Plouzané, France

A. Piola

Servicio de Hidrografia Naval, Buenos Aires, Argentina

W. Zenk

Institut für Meereskunde, Kiel, Germany

Received 8 May 2001; revised 13 July 2001; accepted 4 September 2001; published 26 January 2002.

[1] Three deep anticyclonic eddies of a species only reported once before [Gordon and Greengrove, 1986] were intersected by hydrographic lines of the World Ocean Circulation Experiment (WOCE) and South Atlantic Ventilation Experiment (SAVE) programs in the Argentine Basin. The vortices are centered near 3500 m depth at the interface between North Atlantic Deep Water and Bottom Water. They have ~1500-m-thick cores containing Lower Circumpolar Deep Water and a dynamical influence that may span up to two thirds of the water column. As one eddy was observed just downstream of the western termination of the Falkland Escarpment, a destabilization of the deep boundary current by the sudden slope relaxation is suggested as a potential cause of eddy formation. Besides isopycnal interleaving at the eddy perimeters, strongly eroded core properties in the upper parts of the lenses, associated with low density ratios, hint at double diffusion at the top of the structures as another major decay mechanism. The presence of an eddy in the northern Argentine Basin shows the possibility for a northward drift of the vortices, in this basin at least. Deep events in recent current measurements from the Vema Channel are presented that raise the question of further equatorward motion to the Brazil Basin. *INDEX TERMS*: 4520 Oceanography: Physical: Eddies and mesoscale processes; 4536 Oceanography: Physical: Hydrography; 4576 Oceanography: Physical: Western boundary current; *KEYWORDS*: eddies and mesoscale processes; western boundary currents; hydrography

## 1. Introduction

[2] The oceanic circulation in the western Argentine Basin is characterized by an intense mesoscale variability which is associated, for the most part, with the meandering and eddy-shedding seaward extensions of the Malvinas (Falkland) and Brazil Currents. There have been many studies of this high variability in the upper oceanic layers [e.g., Legeckis and Gordon, 1982; Gordon, 1989; Boebel et al., 1999]. Observations are less numerous in the deep layers, particularly as one moves away from the continental slope, yet Weatherly [1993] presented near-bottom current measurements of nearly a year duration in the abyssal plain that exhibited unusual high levels of eddy kinetic energy ( $>100 \text{ cm}^2 \text{ s}^{-2}$ ) for depths around or  $>5000 \text{ m}$ . From a comparison with Geosat altimeter data, Weatherly et al. [1993] showed that the part of the abyssal variability that had timescales  $>34$  days (the satellite cut-off period) was due to deep extensions of the surface fluctuations. No conclusion could be drawn, however, for the shorter periods which accounted for about half of the near-bottom eddy kinetic energy.

[3] An observation of a deep vortex by Gordon and Greengrove [1986] shows that the abyssal variability in the Argentine Basin has components that differentiate it from the near-surface fluctuations. The reported structure was a lens-shaped eddy at  $46^\circ\text{S}$  and  $400 \text{ km}$  offshore from the continental slope, the density signature of which did not reach upward above  $2500 \text{ m}$ . It contained water that had overflowed at the bottom of the Falkland Plateau. This vortex is, to our knowledge, the only one of its type reported so far. In the

present paper, we describe three structures that are very similar and might be indicative of a significant population in the deep Argentine Basin. Two of the reported eddies were intersected during the World Ocean Circulation Experiment (WOCE) hydrographic section A17 conducted in 1994, and the other one was sampled in 1988 during cruise 4 of The South Atlantic Ventilation Experiment 4 (SAVE-4). The new observations also provide information about the formation mechanism. The proximity of the SAVE-4 eddy to a pronounced change in the continental slope suggests that interaction of the deep Malvinas Current with continental slope irregularities might be a cause of eddy generation. Also presented in this paper are recent near-bottom current measurements at the sill of the Vema Channel that show occasional events that might be related to the deep Argentine Basin vortices. After presenting the new observations in section 2, we analyze several hypotheses relative to the generation of the eddies, their decay, and their fate in section 3. Their possible role at a larger scale is briefly discussed in a concluding section.

## 2. Observations

### 2.1. Eddy Locations and Larger-Scale Environment

[4] The eddy locations are shown in Figure 1a along with the patterns of the Subantarctic Front (SAF) and Subtropical Front (STF) reproduced from Peterson and Whitworth [1989]. The two eddies intersected by A17 (E1 and E2) were found some  $1300 \text{ km}$  apart, one being in the so-called Subantarctic Zone between the SAF and STF (E1 at  $45^\circ35'\text{S}$ ,  $52^\circ27'\text{W}$ ), while the other (E2 at  $35^\circ27'\text{S}$ ,  $45^\circ09'\text{W}$ ) was well inside of the subtropical domain. The vortex described by Gordon and Greengrove [1986] (E3 at  $46^\circ\text{S}$ ,

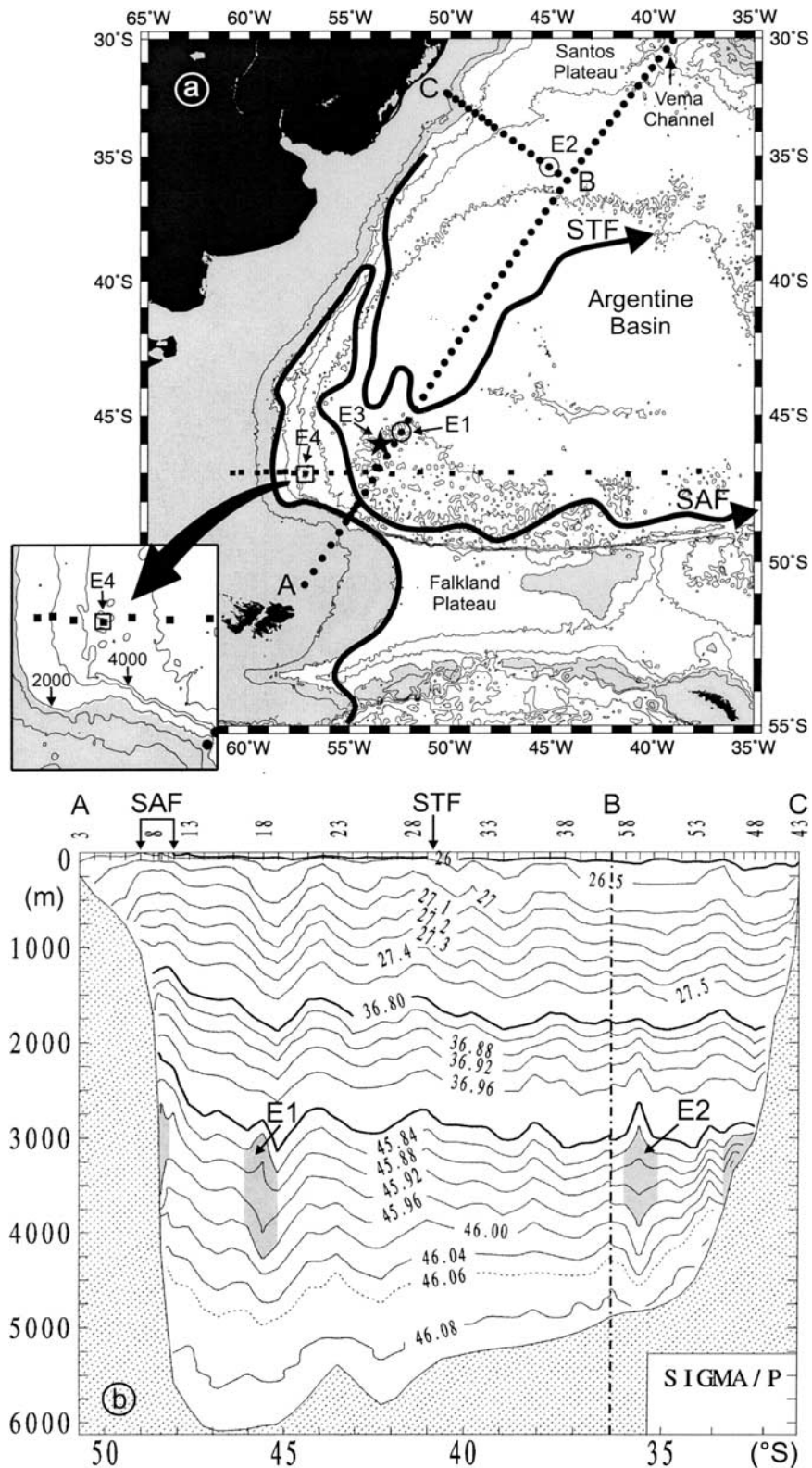


**Figure 1.** (a) Map of the Argentine Basin showing the World Ocean Circulation Experiment (WOCE) A17 (circles) and South Atlantic Ventilation Experiment 4 (SAVE-4) (squares) station positions and the locations of the four studied eddies. Also displayed are the Subantarctic Front (SAF) and Subtropical Front (STF) patterns from *Peterson and Whitworth* [1989]. Bathymetric contours are multiples of 1000 m. The insert shows the change of steepness of the continental slope near 48°S, 57°W. (b) Vertical density distribution along the angled line ABC shown in Figure 1a. Shading (of arbitrary vertical extent) visualizes eddies E1 and E2 and the deep boundary currents near 48°S and 32°S. The SAF and STF locations are reported.

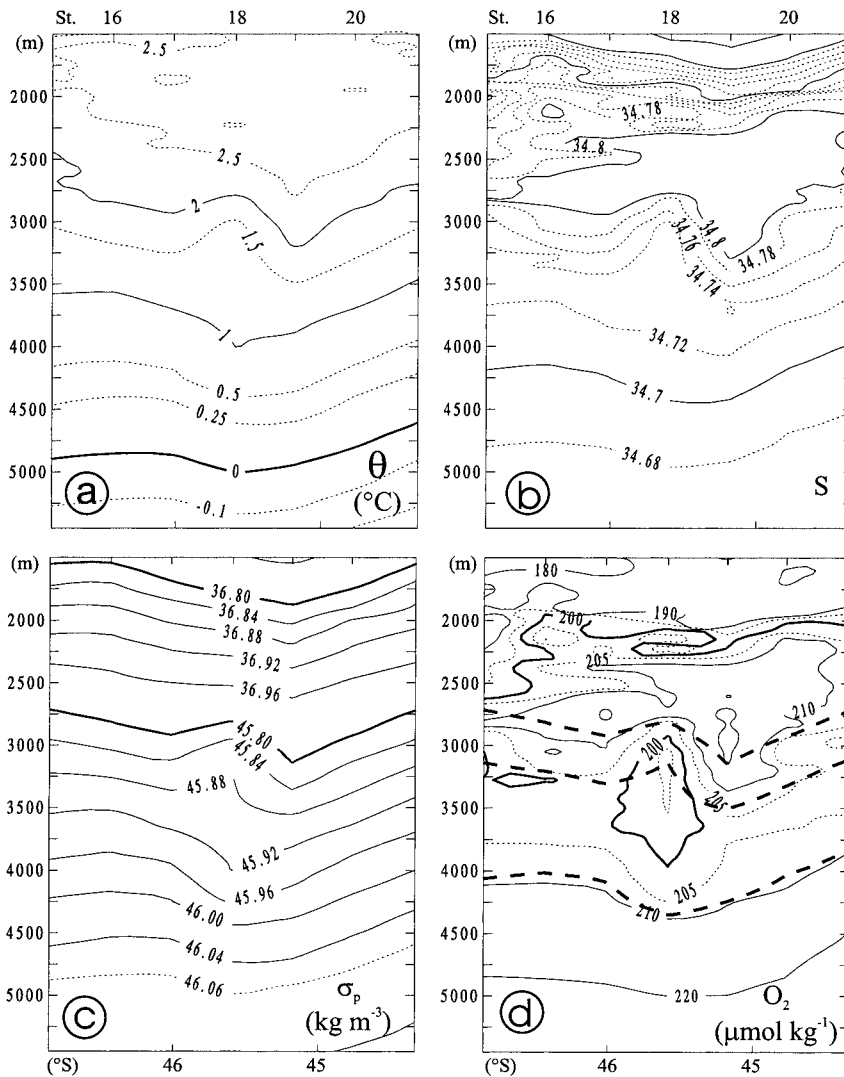


**Figure 2.** Expanded vertical sections of (a) potential temperature, (b) salinity, (c) density ( $\sigma_2$  and  $\sigma_4$ ), and (d) dissolved oxygen showing eddy E1. The bold dashed lines in Figure 2d show the isopycnals  $\sigma_4 = 45.80$ ,  $45.87$ , and  $45.98$ , which were chosen as the upper bound of Lower Circumpolar Deep Water (LCDW), lower bound of North Atlantic Deep Water (NADW), and lower bound of LCDW, respectively.

$53^{\circ}30'W$ ) is in the vicinity of E1, and the SAVE-4 eddy (E4 at  $47^{\circ}03'S$ ,  $57^{\circ}13'W$ ) is near the continental slope in a northward extension of the Polar Frontal Zone delimited by the Malvinas Current and its return flow.

[5] The vertical density section along the angled line ABC (Figure 1b) illustrates the eddies depth-intensified character and relation to the slope currents. The lens-shaped signatures of E1 and E2, typical of anticyclonic structures, are both centered at  $\sim 3500$ – $3600$  m depth in the same density range  $45.88 < \sigma_4 < 45.92$  (the density unit  $\text{kg m}^{-3}$  is omitted in the paper). In Figure 1b this layer shows an important vertical stretching against the steep continental slope that limits the Falkland Plateau to the north (the Falkland Escarpment). Arhan *et al.* [1999a] noted that this stretching is associated with a deep velocity core of the Malvinas Current at  $\sim 3000$ -m depth. They interpreted the sharp density gradient present below this layer against the slope (visible at  $45.92 < \sigma_4 < 46.00$  in Figure 1b) as marking the boundary between the water that has overflowed at the Falkland Plateau and the denser water that comes from farther east along the escarpment. This deep velocity core of the Malvinas Current was seen in the same study to also be present, though in an attenuated form, in the return flow associated with the northeastern limb of the SAF loop. Another

fraction of the deep velocity core is expected to proceed along slope beyond the Malvinas Current retroflection, however, as its density range ( $45.88 < \sigma_4 < 45.92$ ) constitutes the upper part of the Antarctic Bottom Water known to flow equatorward as a western boundary current in the South Atlantic [e.g., Hogg *et al.*, 1999]. At the northern end of the ABC section (Figure 1b) the shoreward shallowing of these isopycnals signals the northern extension.

[6] Because of the important thermohaline variability of the region, there is some ambiguity as to the exact location of the STF along A17. Mémery *et al.* [2000], defining the front from the crossing of the 100-m-depth level by the  $10^{\circ}\text{C}$  isotherm, placed its northernmost intersection with A17 at  $41^{\circ}\text{S}$  (reported in Figure 1b), that is, some  $4^{\circ}$  to the north of the frontal pattern of Peterson and Whitworth [1989]. There are, however, two deep reaching eddies or meanders to the south of this location, which are visible from isopycnal troughs at stations 25 and 19 and which make the A17 snapshot view compatible with the Peterson and Whitworth [1989] pattern. At the time of its sampling the deep eddy E1 looked as if it was integrated in the southern flank of the southernmost of these structures. This suggests that interactions may occur between the anticyclonic deep eddies and the surface-intensified Brazil Current eddies or meanders. This process, called vertical alignment, can

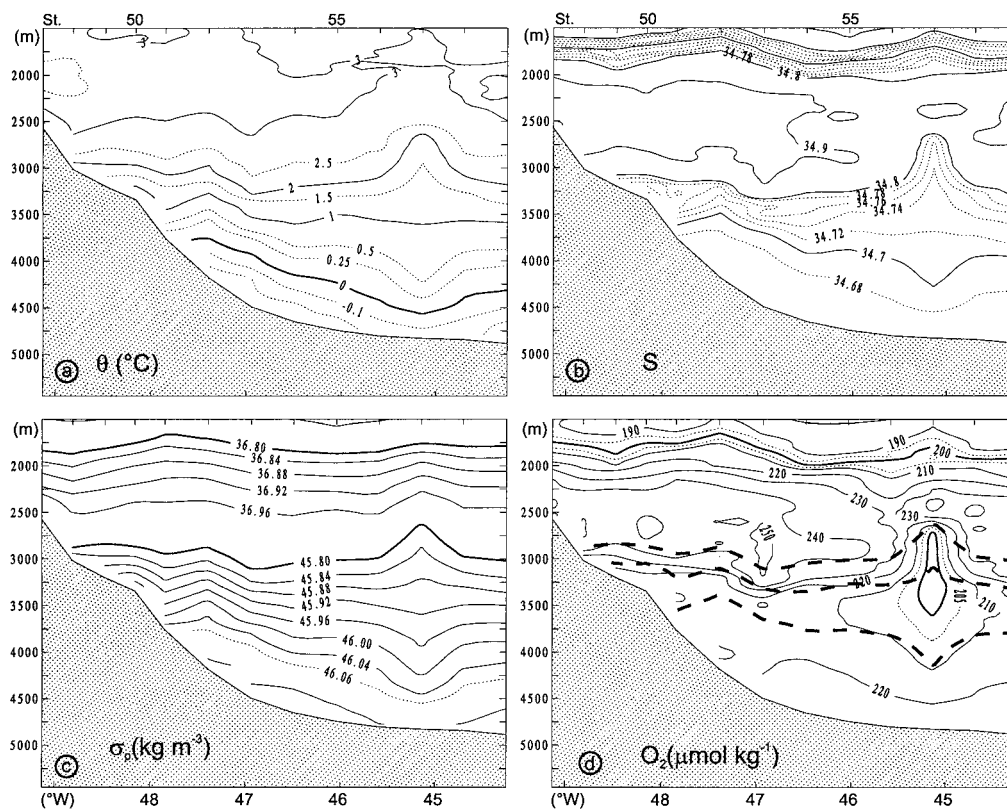


Figure 3. Same as Figure 2 but for eddy E2.

occur for eddies with like-signed vorticity. It was studied by *Polvani* [1991] for equal-size quasigeostrophic vortices with constant potential vorticity and by *Corréard and Carton* [1998] for equal-size vortices with distributed potential vorticity. Both studies showed that alignment is possible when the vortices have a radius larger than the deformation radius and happen to be distant from each other by less than two radii. Both conditions are fulfilled here, with vortex radii of  $\sim 50$  and  $100$  km, clearly larger than the local deformation radius of  $24$  km [*Houry et al.*, 1987], and a distance between the eddy axes that is smaller than the sum of the radii. In the ocean such an alignment process has already been identified between Mediterranean salt lenses in the North Atlantic (meddies) and anticyclones of the Azores Current [*Tychensky and Carton*, 1998].

## 2.2. Comparison of Eddy Properties

[7] For a detailed description and comparison of the eddies we show the vertical distributions of the hydrographic properties of E1, E2, and E4 in Figures 2, 3, and 4, respectively. The corresponding figure for eddy E3 is given by *Gordon and Greengrove* [1986]. The geographical information and core properties of the four eddies are summarized in Table 1. Note that while the potential temperature ( $\theta$ ), salinity ( $S$ ), and density ( $\sigma_4$ ) given for each structure refer to the indicated “sample depth,” the reported oxygen ( $O_2$ ) values are the minimum values in the eddy cores, generally found in the upper parts of the structures. Also reported in Table 1 are the values of the same properties in the deep velocity core against the Falkland Escarpment and in the densest water overflowing at the Falkland Plateau.

[8] Prior to the eddy comparisons, and because of the closeness of E4 to the continental slope, it is useful to give some details on the location of this feature relative to the boundary current. The hydrographic line SAVE-4 intersected the SAF at two locations (Figures 1a, and 4a) that were determined through the crossing of the 200-m-depth level by the  $4^\circ\text{C}$  isotherm [*Peterson and Whitworth*, 1989]. *Peterson* [1992] pointed out that the flow associated

with the western limb of the SAF loop, which constitutes the upper part of the Malvinas Current, is located inshore of the 2000-m isobath. This result is confirmed by the SAVE-4 observations. Figure 4a shows that the center of E4 (station 8) was intersected seaward of the upper Malvinas Current at a distance of  $\sim 130$  km. Below 2000-m depth, and at variance with the situation at the southern end of A17 (Figure 1b), there is no density signature of a deep velocity core at the western end of SAVE-4 (Figure 4c). The vertical thickening of the isopycnal layers around  $\sigma_4 = 45.90$  that was observed right at the boundary in the former section is replaced in the latter by a thinning down shoreward of station 8. It is the lens shape of the deep isopleths around this station (Figure 4a–4c) and the similarity of the water contained in this feature to that of the other eddies (see below) that lead us to regard it also as an eddy.

[9] Figures 2, 3, and 4 and Table 1 reveal close similarities between the core properties of E1, E2, and E4 (e.g.,  $1.0^\circ\text{C} < \theta < 1.2^\circ\text{C}$ ) and slightly greater deviations from those of E3 (e.g.,  $\theta = 0.74^\circ\text{C}$ ). As already seen for the density, the three former have property values that are very close to those of the deep velocity core against the escarpment and are those of the Lower Circumpolar Deep Water (LCDW). To help determine the density range of this water as it enters the Argentine Basin, we show in Figure 5 the  $\theta$ - $S$  and  $\theta$ - $O_2$  diagrams of the A17 station 10 that sampled the deep Malvinas Current (the bold curves in Figure 5). Observing a sharp transition with the overlying Upper Circumpolar Water at  $\sigma_4 = 45.8$  and considering that  $\sigma_4 = 45.98$  is the highest density of the overflow water at the Falkland Plateau (Table 1) [*Arhan et al.*, 2002], we ascribed the interval  $45.80 < \sigma_4 < 45.98$  to the LCDW. When superimposed onto the oxygen distributions of E1 and E2 (Figures 2d and 3d), these isopycnals show that the anomalous water trapped in the eddy cores is formed of the whole LCDW density range and occupies an  $\sim 1500$ -m-thick layer near the centers of E1 and E2. A determination of the isopycnal limits of trapped water from the  $\theta$ - $S$  diagrams of the central and neighboring stations of each eddy (not shown) led to  $45.78 < \sigma_4 < 45.98$ , a

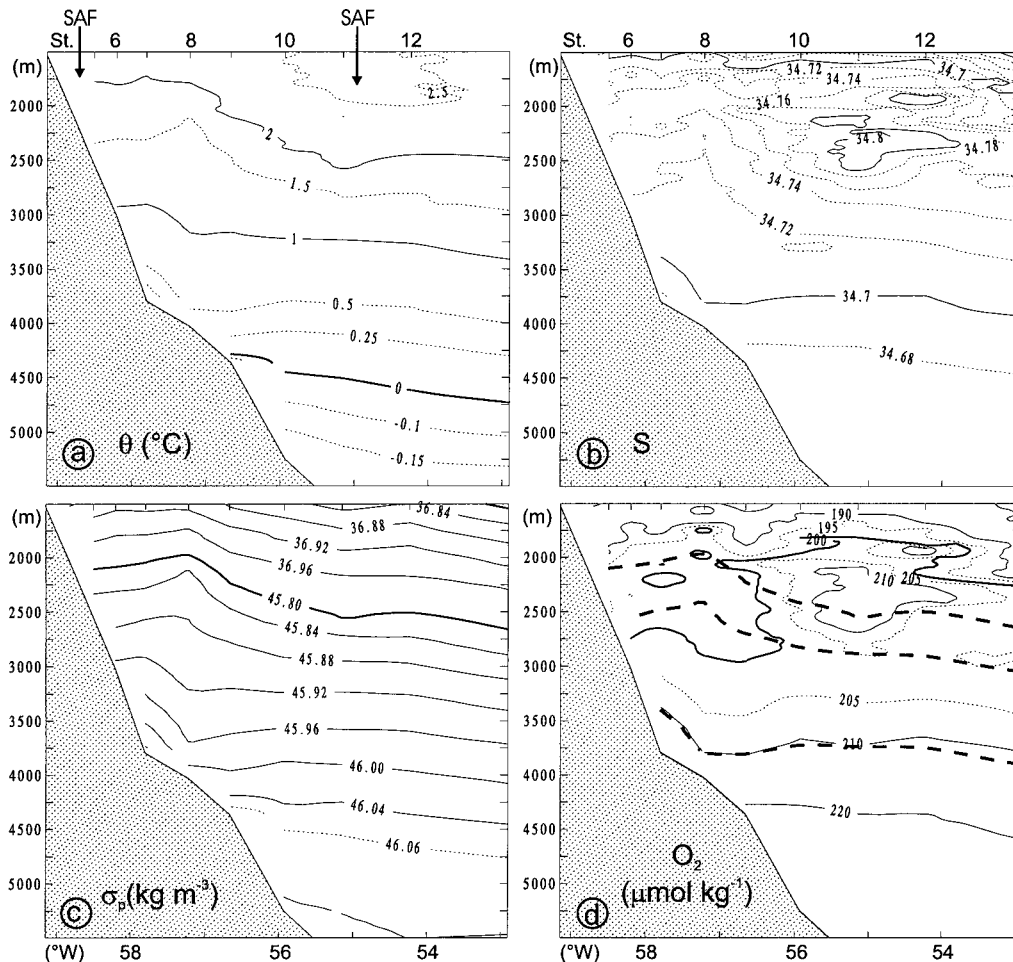


Figure 4. Same as Figure 2 but for eddy E4.

confirmation of the close correspondence with the LCDW density range (isopycnals  $\sigma_4 = 45.78$  and  $\sigma_4 = 45.80$  were only separated vertically by  $\sim 50$  m in E1 and E2).

[10] In the deep Argentine Basin the original density range of LCDW is occupied by diluted North Atlantic Deep Water (NADW) at densities lower than  $\sigma_4 = 45.87$  and by the denser part of the LCDW (named Lower Circumpolar Water by Reid [1989]) below. Reporting the isopycnal  $\sigma_4 = 45.87$  in Figures 2d and 3d (the intermediate dotted line), the eddy cores are observed to straddle the layers of the NADW and of the underlying Lower Circumpolar Water. The  $\theta$ - $O_2$  diagram of the Malvinas Current station in Figure 5b exhibits a regular downward increase of oxygen across the LCDW layer. It is the capping of this downward gradient by the higher values of the NADW that causes the oxygen minima in the upper parts of the eddies (Figures 2d, 3d, and 5b).

[11] Eddy E3, though clearly of the same type as the others from Figure 2 of Gordon and Greengrove [1986], shows slightly different core characteristics that also fall on the LCDW  $\theta$ - $S$  and  $\theta$ - $O_2$  curves (Figure 5) but were found in the Malvinas Current hydrographic profile only 30 m above the lower limit (isopycnal  $\sigma_4 = 45.98$ ) chosen for this water mass. Gordon and Greengrove [1986] pointed out the similarity of the water contained in E3 with that found at the bottom of the Falkland Plateau. Although the E3 values do not match exactly the plateau bottom values from the *Albatross* cruise reported in Table 1, they were, indeed, found at only 90 m above the bottom at the same station. The core properties of the three other eddies were found at shallower levels between 300 and 400 m above the bottom. Similar to what we did for E1 and E2, we used the closed oxygen contours of E3 (from

Figure 2 of Gordon and Greengrove [1986]) to infer the upper isopycnal limit of the anomalous water transported by the eddy. This led to the (approximate) conclusion that, despite the slightly different properties of the inner core, the water entrapped by E3 is also formed of the whole LCDW density range.

### 2.3. Rotational Velocities

[12] Gordon and Greengrove [1986] found a maximum anti-cyclonic velocity of  $8 \text{ cm s}^{-1}$  for E3 using a reference level at the top of the structure. Because of the above mentioned interaction of E1 with a full-depth Brazil Current eddy, referencing the geostrophic velocities at the bottom is probably the best that we can do to estimate the velocities in this vortex. With this choice (Figure 6a) the E1 velocities appear as  $\sim 5 \text{ cm s}^{-1}$  perturbations at depths 2500–5000 m in the full-depth velocity gradient associated with the Brazil Current eddy. The upper and lower bounds of the LCDW are shown in Figure 6 near 3000 and 4200 m depth. An average azimuthal transport of about 3 Sv was estimated for this water mass, using an eddy radius of 55 km equal to the station spacing.

[13] The bottom-reaching density signature of E2 (Figure 1b) suggests that a middepth (rather than bottom) reference level would be more appropriate for this vortex. The velocity profiles referred to 1500-m depth, where the eddy-induced density perturbation vanishes upward, are displayed in Figure 6b. The azimuthal velocities are larger in this structure, with maxima between  $10 \text{ cm s}^{-1}$  and  $15 \text{ cm s}^{-1}$ . The inferred transports in the layer of LCDW trapped by the eddy are 8 Sv southward and 5.6 Sv northward, again assuming a radius of 55 km (4.5 Sv and 4.8 Sv

**Table 1.** Geographical Information and Core Properties of the Eddies<sup>a</sup>

	Falkland Plateau	Boundary Current (A17)	Eddy 1	Eddy 2	Eddy 3	Eddy 4
Latitude	50°42'S	48°27'S	45°35'S	35°27'S	46°S	47°03'S
Longitude	48°31'W	54°27'W	52°27'W	45°09'W	53°30'W	57°13'W
Bottom depth, m	2777	4205	6031	4862	5998	4027
Sample depth, m	2768	3000	3500	3600	3800	3000
$\theta$ , °C	0.574	1.16	1.20	1.00	0.74	1.07
$S$	34.700	34.722	34.723	34.722	34.71	34.715
$\sigma_4$ , kg m <sup>-3</sup>	45.98	45.894	45.89	45.91	45.96	45.904
O <sub>2</sub> minimum, $\mu\text{mol kg}^{-1}$	204	<197	193	195	200 (4.6 mL L <sup>-1</sup> )	196
Cruise and source	ALBATROSS [Heywood and Stevens, 2000]	CITHER-2 [Groupe CITHER-2, 1995]	CITHER-2, 1995]		Atlantis II-107 [Gordon and Greengrove, 1986]	SAVE-4 [Scripps Institute of Oceanography, 1992]

<sup>a</sup>For comparison, the first two columns give the same information for the water of highest density at the bottom of the Falkland Plateau and in the core of LCDW in the Malvinas Current. The eddy 3 values are from Table 1 of Gordon and Greengrove [1986] with the following two differences: The oxygen value is the core minimum, instead of the value at the sample depth; the density value is expressed using the international equation of state EOS80.

with a bottom reference level). Such values are comparable with an estimate of 6 Sv for the transport of LCDW in the deep Malvinas Current [Arhan *et al.*, 1999a]. The azimuthal velocities are not limited to the core of anomalous water, however. The eddy density signature and our ensuing choice of reference level suggest that more than two thirds of the water column are affected by the eddy velocities. At the bottom, currents of the order of  $5 \text{ cm s}^{-1}$  induced by such vortices might be a contribution to the abyssal low-frequency variability observed by Weatherly [1993] that we mentioned in section 1. The total anticyclonic transport below 1500-m depth by this eddy was estimated at 16 Sv in the southward direction and 10 Sv in the northward direction.

[14] Probably because of its proximity to the continental slope, E4 was tilted with respect to the horizontal when observed. Because of this asymmetry, no single reference level valid for the whole structure could be chosen, and no geostrophic computation was made for this eddy.

### 3. Hypotheses on the Generation, Decay, and Fate of the Eddies

#### 3.1. Eddy Generation

[15] Having emphasized the similarities of the core properties in E3 with those of the bottom water at the Falkland Plateau,

Gordon and Greengrove [1986] hypothesized a generation at the plateau and subsequent isopycnal spreading into the Argentine Basin. The additional descriptive elements presented in section 2 suggest that a detachment from the deep Malvinas Current might be another possible mechanism. This hypothesis is supported by the observation that the density range and other properties of the anomalous water trapped in eddies 1, 2, and 3 are similar to those of the deep velocity core of LCDW in the Malvinas Current (Figures 1–3). While the proximity of E1, E3, and E4 to the southwestern corner of the Argentine Basin suggests a detachment in this region, the different location of E2 (Figure 1a) raises the question of vortex generation at more northern latitudes. For an answer to this question we observed that mixing causes an equatorward increase of LCDW oxygen concentrations along the continental slope and compared the minimum oxygen value in E2 ( $195 \mu\text{mol kg}^{-1}$ ) to available data near the boundary. A section at  $38^\circ\text{S}$  [Maamaatuaiahutapu *et al.*, 1992] near the tip of the Malvinas Current loop (Figure 1a) shows near-slope oxygen concentrations already in excess of  $208 \mu\text{mol kg}^{-1}$  ( $4.8 \text{ mL L}^{-1}$ ) at this latitude. If E2 was detached from the boundary flow, the separation therefore certainly took place to the south of the current retroflexion.

[16] One may think of several dynamical mechanisms for the detachment of eddies from the deep Malvinas Current. The sharp seaward density gradient at the base of the LCDW core in this

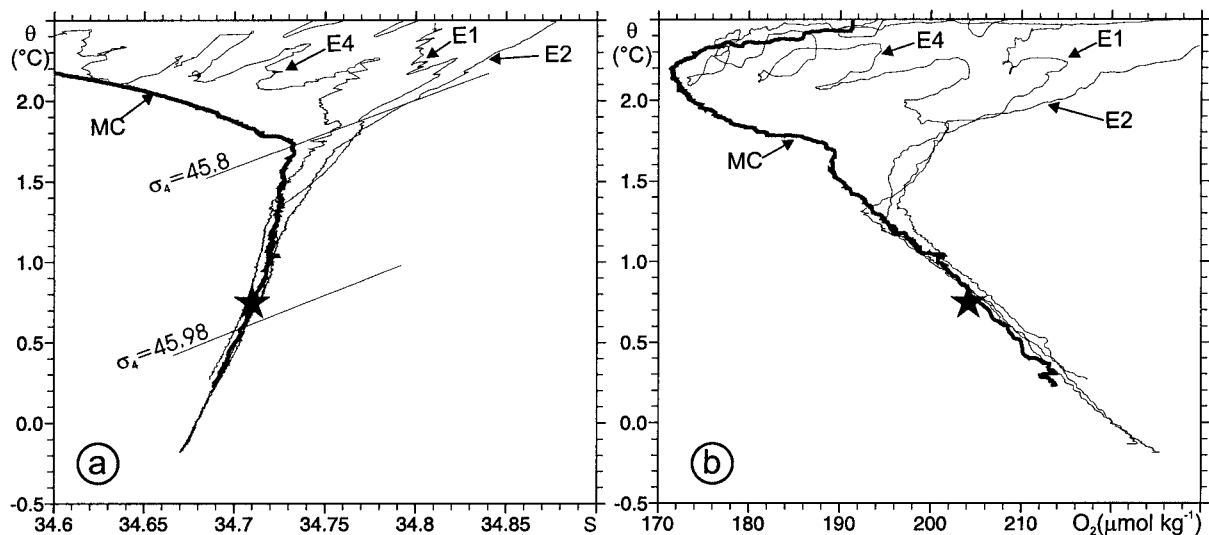


**Figure 5.** Deep (a)  $\theta$ - $S$  and (b)  $\theta$ - $O_2$  diagrams in the Malvinas Current (MC) (A17 station 10) and in eddies E1, E2, and E4. Isopycnals  $\sigma_4 = 45.8$  and  $\sigma_4 = 45.98$  show the LCDW density range. The stars show the core properties of eddy E3 described by Gordon and Greengrove [1986].

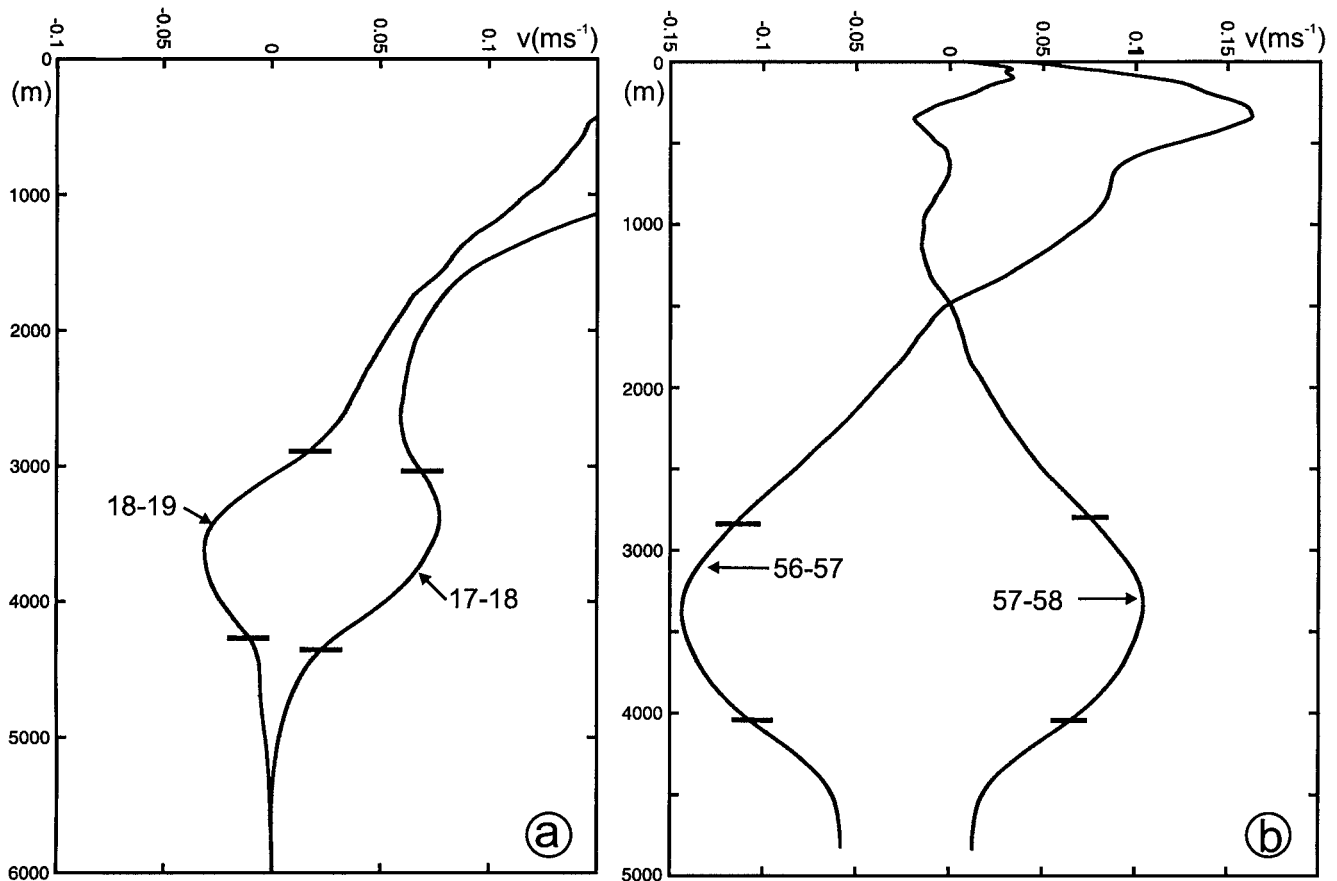


**Figure 6.** Geostrophic velocity profiles of eddy E1 (a) referenced to the bottom and eddy E2 (b) referenced to 1500-m depth. The A17 station pair numbers are indicated, and velocities are positive eastward in Figure 6a and northward in Figure 6b. The short lines across the profiles show the limits of the LCDW layer.

current (Figure 1b) is associated with a downward velocity decrease of  $\sim 10 \text{ cm s}^{-1}$  from 3000 to 3800-m depth that could generate baroclinic instability. However, simple calculations with a three-layer Phillips model [Quiniou, 2000] showed that baroclinic instability for the deep Malvinas Current was associated with very long waves (600 km wavelength) over a flat bottom and that the current was stabilized by a northward deepening bottom. An assumption in this simple model was to keep the same averaged current width over flat and sloping bottoms. Under this condition at least, baroclinic instability could not generate the deep eddies.

[17] The proximity of the Malvinas Current to the opposite return current in this region (Figure 1a) is associated with a lateral shear that might cause barotropic instability. A three-layer quasigeostrophic model was also used by Quiniou [2000] to assess the barotropic instability of a coastal jet with piecewise-constant potential vorticity. This linear calculation did not lead to a significant growth rates nor to realistic wavelength. Though simple, this model again does not point toward barotropic instability as a likely mechanism for the generation of the deep eddies.

[18] The closeness of E4 to the continental slope suggests that this structure had just separated from the continental slope when observed. This hints at a possible role of topographic irregularities in the generation mechanism, as E4 was observed at a short distance downstream of a sharp variation in the continental slope steepness, which marks the western termination of the Falkland Escarpment (see insert of Figure 1a). The change is particularly pronounced in the depth range 2000–4000 m, which is the approximate layer of the Malvinas Current LCDW velocity core

(Figure 1b). Considering this depth interval, the steepness decreases from 0.08 along A17 to 0.02 along SAVE-4. The steepness decrease is less important, yet still pronounced, when estimated in the interval 1000–5000 m (from 0.04 to 0.016). A current destabilization by sudden slope relaxation appears to us the most probable mechanism for the formation of E4 and a possible one for the other eddies. A simple budget model following Warren [1969], given in Appendix A, indicates that a current with dimensions and amplitude typical of the deep Malvinas Current which originally flows westward against a zonal vertical wall can undergo a doubling in width after encountering a northward deepening bottom slope of 0.02. This formation of a bulge (or meander), by violating the condition of equal width upstream and downstream of the isobath divergence used by Quiniou [2000] in his Phillips model (see above), might trigger baroclinic instability and lead to vortex detachment.

[19] The possibility for eddy generation at the Falkland Escarpment termination does not exclude other formation sites. The resemblance of the E3 core properties to the near-bottom characteristics at the Falkland Plateau, which was not observed for the other structures, might indicate a formation nearer the sill of the plateau, as suggested by Gordon and Greengrove [1986]. Arhan et al. [2002] showed that the flow of LCDW present in the deep Malvinas Current crosses the plateau some 250 km to the east of the SAF and joins in the boundary current at only a short distance upstream of the A17 track. Whether instabilities of the overflow current or this addition of a deep component to the boundary flow could be associated with occasional eddy shedding should also be examined. More generally, and assuming that the boundary transport is not constant with time, the formation of isolated blobs of

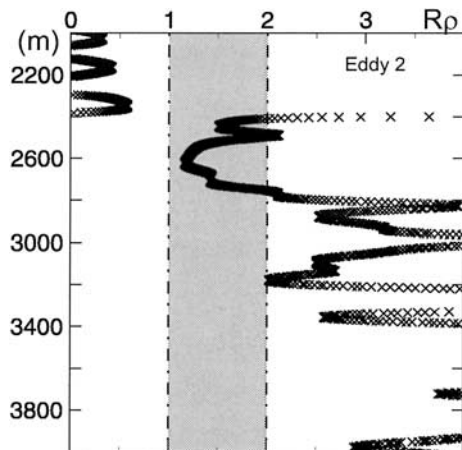


**Figure 7.** Profile of the density ratio  $R_p$  (estimated using vertical steps of 50 m) in the upper core eddy E2. The vertical lines at  $R_p = 1$  and  $R_p = 2$  bound the domain favorable to salt fingering.

water from a pulsating current was also shown to be possible by *Nof* [1991].

### 3.2. Eddy Erosion

[20] As the dynamic signature of the vortices is associated with the presence of an anomalous water mass in the eddy cores, the gradual erosion of the anomalous properties by mixing will be a factor of eddy decay. A first mixing process that is suggested by the vertical distributions of properties (Figures 2, 3, and 4) and that could be more clearly detected from the  $\theta$ - $S$  diagrams at the eddy borders (not shown) is isopycnal interleaving with the adjacent water masses, particularly with NADW that surrounds the structures at densities lower than  $\sigma_4 = 45.87$ . The phenomenon was also visible at higher densities, though in an attenuated form, between the unmixed LCDW of the eddy core and the surrounding more diluted version of the same water mass. *Armi et al.* [1989], in a study of the decay of a Mediterranean salt lens in the North Atlantic (a Meddy), concluded that this mechanism was responsible for the largest fraction of the net mixing of the structure. Its effect was to erode the eddy from its edges, thus reducing the diameter but leaving the properties near the eddy axis unchanged until the thermohaline intrusions had reached the center. A similar behavior is to be expected for the abyssal eddies of the Argentine Basin, with the difference that greater erosion occurs in the upper part of the structure because it is surrounded by a more contrasted water mass (NADW), than in the lower part. The pear-shaped oxygen distribution of E2 (Figure 3d), associated with a decrease of the eddy diameter at densities lower than  $\sigma_4 = 45.87$ , might be related to this phenomenon.

[21] Lateral erosion at the eddy rims does not seem to be the only mixing mechanism, if one compares the  $\theta$ - $S$  and  $\theta$ - $O_2$  diagrams at the eddy central stations with those of the LCDW in the Malvinas Current (Figure 5). In E1, E2, and E4 we observe that while the lower parts of the cores keep the original water mass properties, the upper parts have become saltier and more oxygenated than at the corresponding densities in the Malvinas Current. These modifications near the eddy centers with no trace of interleaving are unlikely to result from lateral mixing at the eddy perimeters. They most certainly reflect vertical mixing with the overlying NADW. In Figure 5 we note that the deviations from the original property diagrams are lowest for E4 and highest for E2 which are the least and most distant structures, respectively, from an assumed location of origin at the southern boundary of the Argentine Basin.

[22] The positive vertical gradients of temperature and salinity at the LCDW-NADW transition on top of the eddy cores suggest

double diffusion in the salt-fingering regime as a possible mechanism for vertical mixing. *Schmitt* [1981] pointed out that the mixing rate associated with salt-fingering convection in the ocean is only significant for values of the density ratio  $R_p = \alpha T_z / \beta S_z$  between 1 and 2, with an increase toward  $R_p = 1$  (where  $\alpha$  and  $\beta$  are the thermal expansion coefficient and haline compression coefficient, respectively). Computation of the  $R_p$  profiles from E1 and E2 showed this to be the case in the upper parts of the eddy cores, with values as low as 1.16 in E2 (Figure 7). In other eddy species, salt fingering has been more frequently observed at the bottom of the structures than at their top. *Armi et al.* [1989] showed that the undersides of Meddies are also unstable to salt-fingering convection, with density ratios around  $R_p = 1.5$  and the presence of thermohaline steps that often characterize this mechanism. Salt fingering at the base of an Agulhas ring was also detected, with density ratios as low as  $R_p = 1.2$  and thermohaline staircases [*Arhan et al.*, 1999b], but in that case the process is thought to be active only at the beginning of the rings lives in structures that have been modified by air-sea interaction in the formation region. Salt fingering should have a more important effect on the eddies we are studying here, for, as they propagate northward, these structures are overlaid by more and more saline NADW. This, by maintaining low density ratios in the eddies upper cores, will keep the salt-fingering process active. The low  $R_p$  values found in E2, which is thought to be the farthest from the formation region, and the significant core property modifications revealed by Figure 5 corroborate the idea of a mixing process that remains active on the old structures.

[23] If we take for granted that eddies E1 and E2 originated at the southern boundary of the Argentine Basin, rough estimates of the eddy drift speeds inferred from Figure 6 provide an order of magnitude for the ages of the structures. *Flierl* [1981] showed that trapping of water occurs in an eddy at depths where the horizontal maximum azimuthal velocity exceeds the drift speed of the structure. Above and below this domain the water is set in motion at the passage of the eddy but not entrained in it. The vertical limits of trapped water reported on the velocity profile of Figure 6 suggest approximate drift velocities of  $2.5 \text{ cm s}^{-1}$  for E1 and  $8 \text{ cm s}^{-1}$  for E2. The high estimate found for the latter vortex might be partly due to an advection by the abyssal equatorward boundary current. Taking 450 km and 1700 km for the distances of E1 and E2 to their formation region, ages of 7 months and 8 months were found. These values are admittedly very crude approximations only indicative of possible life durations of the order of 1 year for such structures.

### 3.3. Fate of the Deep Eddies

[24] Looking back at Figure 1a, we observe that E1, E2, and E3 were all observed on the equatorward side of the cyclonic loop described by the SAF in the southwestern Argentine Basin. Associated with the northeastern limb of this loop is the Malvinas return current that extends downward to  $\sim 4000 \text{ m}$  depth [*Arhan et al.*, 1999a], with velocities of the order of  $5 \text{ cm s}^{-1}$  in the LCDW layer. With an eddy generation at the southern boundary of the Argentine Basin a crossing of this deep current by the vortices in the course of their northward motion is required. Considering the above-quoted magnitude of the current and the rotational velocities of the eddies (Figure 6), a crossing seems possible if we apply a simple dynamical criterion derived by *Vandermeersch et al.* [1998] for the crossing of a zonal jet by a vortex. This criterion indeed states that the swirl velocity must be at least equal in amplitude to the maximum jet speed for crossing to occur, which is satisfied here.

[25] In section 2 we noted the apparent trapping of E1 in the deep part of a Brazil Current eddy and attributed this situation to a vertical alignment process between the two structures. Although Brazil eddies may drift southeastward in the Subantarctic Zone [e.g., *Legeckis and Gordon*, 1982], the one which contained E1 at



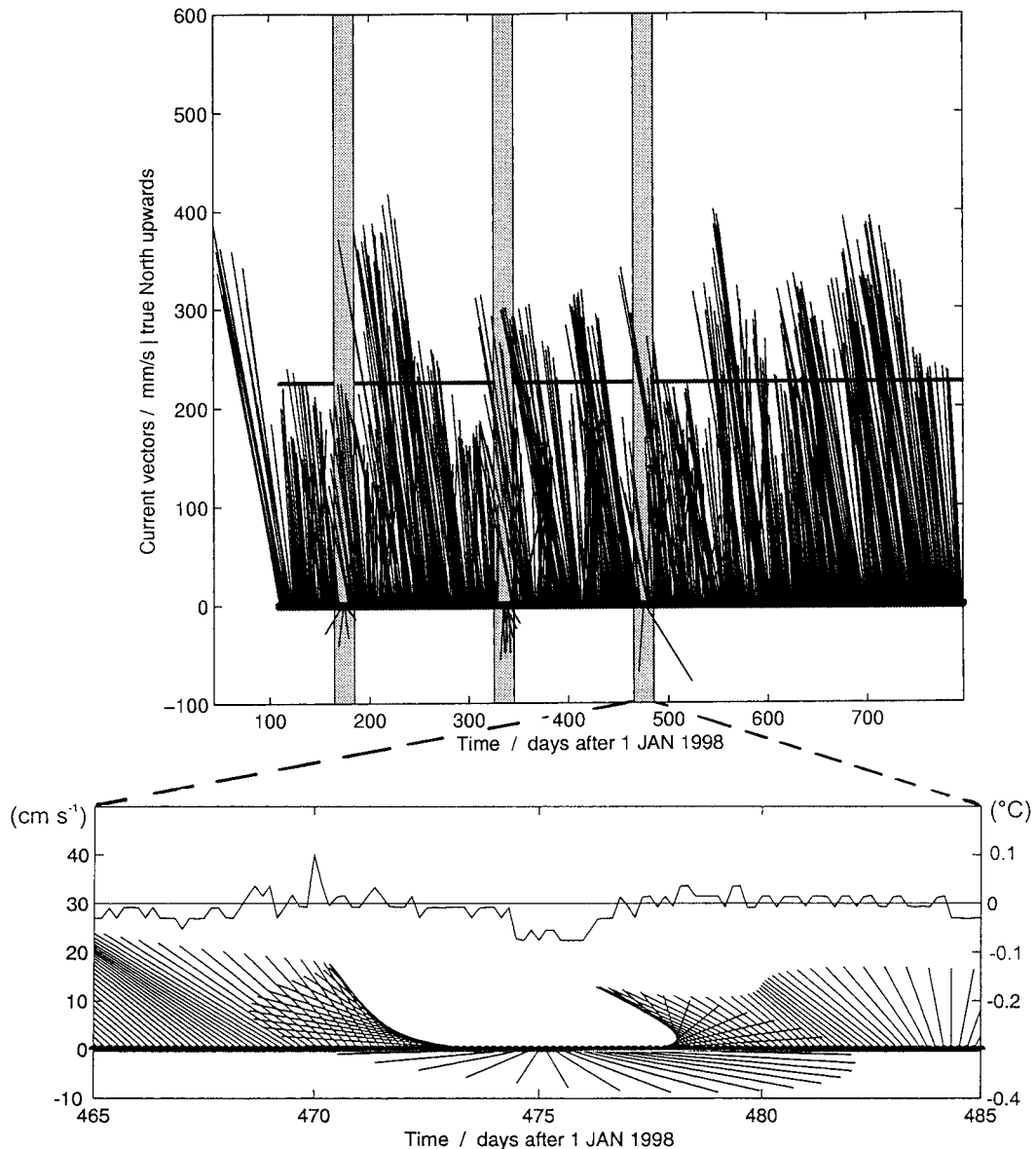


**Figure 8.** (a) Vector time series (true north upward) from mooring V389 on the eastern flank of the Vema Sill ( $31^{\circ}14'S$ ,  $39^{\circ}20'W$ ). The instrument recorded at a depth of 4310 m (bottom distance 270 m). The horizontal bar marks the mean speed of the whole time series. The three vertical strips label intervals with conspicuous current reversals in the otherwise consistent northward flow pattern of Lower Circumpolar Deep Water. This water mass is exported from the Argentine Basin into the Brazil Basin. (b) Zoom on the third reversal event (see Figure 8a) displayed as a 4-hour low-pass-filtered vector sequence. Concurrent in situ temperature fluctuations show an associated negative temperature anomaly (relative to the total mean estimate of  $0.33 \pm 0.05^{\circ}C$ ).

the time of A17 was shown through altimetric tracking [Béranger, 1997] to return to the subtropical domain  $\sim 2$  months after we intersected it. This therefore appears as a means by which the deep eddies can be conveyed to the subtropical domain.

[26] Gordon and Greengrove [1986] noted that if E3 continued to move northward along isopycnals, its core would only intersect the seafloor near  $10^{\circ}N$ . Our observation of E2 at  $35^{\circ}27'S$  shows that northward propagation is a reality in the Argentine Basin, yet we expect that further equatorward motion will be impeded by two obstacles even before the eddies can reach the Brazil Basin. The first obstacle is a deep thermohaline front observed near  $34^{\circ}S$  along A17 [Mémery *et al.*, 2000] at the boundary between LCDW and NADW just detached from the deep western boundary currents. The eastward current associated with this front has an averaged amplitude of  $\sim 2.5 \text{ cm s}^{-1}$  at the depth of the eddy cores

[Hogg *et al.*, 1999]. Resorting again to the dynamical criterion of Vandermeersch *et al.* [1998], a crossing of this current by eddies like E2 and E3 is possible. Once the eddies have crossed the deep front near  $34^{\circ}S$ , however, we expect from the above discussion on mixing that the increased NADW concentration to the north of the front would accelerate their erosion.

[27] The other obstacle on the way of the eddies to the Brazil Basin is naturally the Rio Grande Rise. When observed, the denser part of E2 ( $\sigma_4 > 45.87$ ) was indeed embedded in the western boundary current that carries bottom water northward to the Brazil Basin via the Vema Channel. As the bottom densities in the channel ( $\sigma_4 > 46.07$  [Speer and Zenk, 1993]) and over the deep Santos Plateau to the west of it ( $\sigma_4 = 46.03$  [Hogg *et al.*, 1999]) exceed those of the eddy cores, the Rio Grande Rise does not stand as a physical barrier to farther northward motion, even though

interaction with the bathymetry is to be expected. We examined several hydrographic sections in the vicinity of the Vema Channel and Santos Plateau in a search for deep lenses of homogeneous water. The only structure that showed similarities with the Argentine Basin ones was found at another A17 station downstream of the channel (28°32'S, 37°39'W). Although the core temperature of this lens was also  $\theta = 1.0^\circ\text{C}$ , the other parameters ( $S = 34.78$ ,  $\text{O}_2 = 235 \mu\text{mol kg}^{-1}$ , and  $\sigma_4 = 45.96$ ) reflected a much greater NADW influence than in the Argentine Basin structures, and the eddy  $\theta$ - $S$  diagram was identical to those of the surrounding water. The latter observation hints at a local formation.

[28] We also examined current times series from the Vema Channel and show in Figure 8 measurements from a recent mooring at 31°14'S, 39°20'W in the eastern part of the central Vema Sill [Zenk *et al.*, 1993]. This mooring was recovered by FS Meteor on March 8, 2000, after 686 days recording time. Among other self-recording instruments it carried one current meter near the base of the LCDW stratum at 4310-m depth or 270 m above the ocean bottom. Prior to a more extensive analysis of this new data set, we have selected one vector time series that may be relevant to this discussion on the fate of the deep eddies.

[29] Figure 8a shows a series of 4-hour current vectors representing the northward throughflow of LCDW across the sill. On average, a rather high mean advection down in the deep Vema Channel ( $22.5 \text{ cm s}^{-1}$ ) lies in the expected range that previous long-term observations by Hogg *et al.* [1982] and Tarbell *et al.* [1994] have revealed. The series, however, depicts three obvious anomalies where the deep flow reverses (shaded vertical strips in Figure 8a). Within 8232 samples we counted 199 cases with a southward component, which represent a sum time slot of only 2.4% of the total time series. Figure 8b, which contains a more detailed view of the third reversal event in Figure 8a, demonstrates a perturbation of roughly 1 week duration that is associated with a temperature drop of barely  $0.1^\circ\text{C}$ . The first event in Figure 8a is similar in duration and temperature anomaly, and the center event is about twice as long with no clear simultaneous temperature anomaly. All three events imply sudden anticlockwise rotations of the velocity that could be caused by northward drifting eddies. We stress, however, that these measurements are not in themselves a proof that deep eddies such as E2 can move northward along the Vema Channel, as other causes of current reversal exist, particularly in the eastern part of the Channel [Hogg *et al.*, 1982]. We present them as a possible clue deserving further examination.

[30] We found another event signature in measurements above the eastern part of the Santos Plateau, at 30°35'S, 40°47'W [Tarbell *et al.*, 1994], where the water depth is  $\sim 3700$  m. The only available time series in this mooring, at a depth of 2600 m, also shows an anticlockwise velocity rotation over a few days, with magnitudes in excess of  $10 \text{ cm s}^{-1}$ , associated with a negative temperature anomaly. Here also we can only note the compatibility with a possible northward motion of a deep eddy.

[31] Finally, another region for possible subsequent eddy motion would be farther east in the Argentine Basin, particularly as a fraction of the abyssal boundary current, that does not proceed to the Brazil Basin, turns eastward in the northern part of the basin [Reid, 1989]. An examination of hydrographic transects in that region did not provide other observations, however.

#### 4. Summary and Conclusion

[32] Gathering the observations from the SAVE-4 and WOCE A17 hydrographic lines suggests that the western Argentine Basin might be at any time populated by a significant number of deep eddies of the species originally described by Gordon and Greengrove [1986]. This, of course, needs confirmation, and estimates of this population and of the main eddy trajectories will be required in order to assess their role at the basin scale. With only a few

occasional observations at our disposal we are not at a stage when this can be envisaged. As these structures occupy a density layer that straddles those of the NADW and LCDW, however, we may already expect an influence on the larger-scale transports and mixing of these water masses.

[33] Large-scale studies of the deep circulation of the South Atlantic [e.g., Reid, 1989] suggest that a part of the NADW that is conveyed to the Argentine Basin by the southward deep western boundary current is subject to mixing with deep circumpolar water in this basin before returning northward through the ocean interior in a diluted form. Isopycnal interleaving of the two water masses in the NADW density range ( $\sigma_4 < 45.87$ ) is certainly a major mixing process [Georgi, 1981]. Figures 4b and 4d show this mechanism to be active at the boundary (near 56°W) between E4 and the return flow of the Malvinas Current influenced by NADW characteristics. From our observations, double diffusion at the top of the eddies is another process contributing to the dilution of the NADW. Finally, the role of the vortices in mixing does not reduce to the progressive dilution of their anomalous core properties in the background water of the Argentine Basin. Figure 6b suggests that their stirring effect may reach upward to  $\sim 1500$ -m depth throughout the NADW and into the Upper Circumpolar Water and downward to the bottom through the Weddell Sea Water.

[34] Although a part of the deep Malvinas Current retroflects at the Malvinas-Brazil confluence near 38°S (Figure 1a), another part is known to proceed equatorward along the continental slope underneath the deep southward boundary current of NADW [Reid *et al.*, 1977]. This extension of the abyssal boundary current is the main route by which LCDW (at densities higher than  $\sigma_4 = 45.87$ ) and Weddell Sea Deep Water are injected in the subtropical domain of the South Atlantic. Our observation of E2 to the north of the STF suggests that the shedding and northward motion of abyssal eddies is another mechanism of LCDW transfer to the subtropical domain. We note, however, that the denser part of E2 was in the northward boundary flow when observed, so that this current itself may facilitate the equatorward drift of the structures.

[35] In section 3 we presented hypotheses relative to the generation, decay, and fate of the deep eddies, confirmation of which would certainly require additional measurements or model studies. The exact correspondence of the core densities with those of the LCDW in the deep Malvinas Current and the observation of E4 just downstream of the Falkland Escarpment termination suggest a destabilization of the deep slope current by the sudden bathymetric relaxation. However, the possibility of eddy generation at the location upstream of A17 where the core of LCDW joins in the Malvinas Current and the effects of a pulsating character of the current [Vivier and Provost, 1999] should also be examined. Vertical mixing at the top of the lenses, probably caused by double diffusion, was suggested as a factor of erosion of the eddy core properties. This process should be all the more effective as double diffusion will be favored by a northward motion of the structures at the lower boundary of more and more saline NADW. The possibility for the vortices to proceed to the Brazil Basin over the deep Vema Channel and the Santos Plateau is another intriguing issue, especially as current measurements in this region show events that could be the signatures of such passages.

#### Appendix A:

[36] Strong simplifications of the bathymetric configuration and vertical structure of the deep Malvinas Current are made here to follow fairly closely Warren's [1969] theory of current branching over divergent isobaths. The flow is assumed to be barotropic shallow water. The model continental slope is zonal, with a westward flowing boundary current against it. Upstream of the isobath divergence the Falkland Escarpment is represented by a vertical wall, and the bottom is flat (Figure A1a). In this region the flow has a width  $L$ , thickness  $H$ , and velocity  $U$ . Downstream of

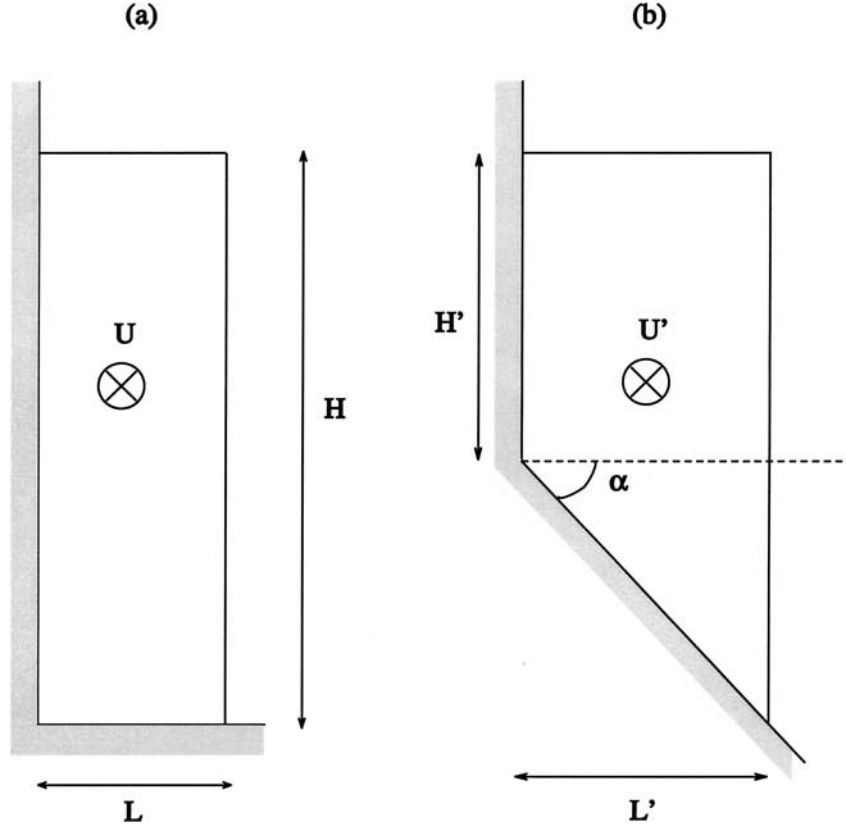


**Figure A1.** Schematized current cross sections used to estimate the increase of the current width resulting from a divergence of the isobaths, with definitions of the notations used in the text. (a) Upstream of the isobath divergence, (b) Downstream of the isobath divergence.

the divergence, the current flows over a sloping bottom which cuts it on part of its height; the bottom slope is  $\alpha$  (Figure A1b). There the current width is  $L'$ , its thickness at the coast is  $H'$ , and its velocity is  $U'$ . We also set  $L' = L + dL$ ,  $U' = U + dU$ ,  $H_0 = H' - \alpha L/2$ , and  $\Delta H = H_0 - H$ .

[37] The model equations ensure transport and potential vorticity conservation. The latter is integrated from the coast to the offshore boundary of the current which is a transport streamline. These two conservation equations are written:

$$T = \int_0^1 h u dy,$$

where  $y$  is the northward coordinate,

$$f_0 T/h + u^2/2 = \text{const},$$

where  $T$  is the constant transport and  $h$ ,  $u$ , and  $l$  are the local values of thickness, velocity, and width, respectively. Here  $f_0$  is the Coriolis parameter.

[38] These two expressions are evaluated both at the upstream and downstream locations. We obtain for the conservation of transport

$$U L H = (U + dU)(L + dL)(H_0 - \alpha dL/2)$$

and for the potential vorticity equation

$$dU = f_0 L (H_0^2 - H H_0 - \alpha H dL/2) / H_0^2,$$

leading to the final relation

$$dL = -\Delta H U L [(f_0 L/U) + 1] / [U(H_0 - \alpha L/2) - f_0 L^2 \alpha H / 2 H_0].$$

[39] Assuming that  $H = 1500$  m, the approximate thickness of the LCDW velocity core at the escarpment (Figure 1a), with  $H' = 500$  m,  $L = 35$  km,  $U = -0.10$  m s<sup>-1</sup>,  $f_0 = -10^{-4}$  s<sup>-1</sup>, and  $\alpha = -0.02$ , we obtain  $dL = 36$  km that is a doubling of the current width downstream of the isobath divergence.

[40] **Acknowledgments.** The participation of M.A. in this work was supported by IFREMER (grant 210161) and INSU/CNRS in the framework of the Programme National d'Etude de la Dynamique du Climat (PNEDC). The work relative to mooring V389 was supported by the Deutsche Forschungsgemeinschaft, Bonn. In Germany, WOCE was also funded by the Bundesministerium für Bildung und Forschung, Berlin. We are grateful to K. Heywood and D. Stevens for allowing us to refer to the recent ALBATROSS data at the Falkland Plateau. We also thank two anonymous reviewers whose comments helped us improve the manuscript. We acknowledge the help of P. Le Bot for the preparation of the manuscript. This is a contribution to the World Ocean Circulation Experiment.

## References

- Arhan, M., K. J. Heywood, and B. A. King, The deep waters from the Southern Ocean at the entry to the Argentine Basin, *Deep Sea Res., Part II*, 46, 475–499, 1999a.
- Arhan, M., H. Mercier, and J. R. E. Lutjeharms, The disparate evolution of three Agulhas rings in the South Atlantic Ocean, *J. Geophys. Res.*, 104, 20,987–21,005, 1999b.
- Arhan, M., A. C. Naveira Garabato, K. J. Heywood, and D. P. Stevens, The

- Antarctic Circumpolar Current between the Falkland Islands and South Georgia, *J. Phys. Oceanogr.*, in press, 2002.
- Armi, L., D. Hebert, N. Oakey, J. F. Price, P. L. Richardson, H. T. Rossby, and B. Ruddick, Two years in the life of a Mediterranean salt lens, *J. Phys. Oceanogr.*, 19, 354–370, 1989.
- Béranger, I., Remplacement de sections hydrographiques dans leur contexte spatio-temporel grâce aux données satellitaires, Rapport de stage ENSIE-TA, document 1, 48 pp., document 2, 40 pp., Ecole Natl. Supér. Ing. des Etudes et Tech. d'Armement, Brest, France, 1997.
- Boebel, O., C. Schmid, and W. Zenk, Kinematic elements of Antarctic Intermediate Water in the western South Atlantic, *Deep Sea Res., Part II*, 46, 355–392, 1999.
- Corréard, S., and X. Carton, Vertical alignment of geostrophic vortices, in *Simulation and Identification of Coherent Structures in Flows*, pp. 191–200, Kluwer Acad., Norwell, Mass., 1998.
- Flierl, G. R., Particle motions in large-amplitude wave fields, *Geophys. Astrophys. Fluid Dyn.*, 18, 39–74, 1981.
- Georgi, D. T., On the relationship between the large-scale property variations and fine structure in the Circumpolar Deep Water, *J. Geophys. Res.*, 86, 6556–6566, 1981.
- Gordon, A. L., Brazil-Malvinas confluence—1984, *Deep Sea Res., Part A*, 36, 359–384, 1989.
- Gordon, A. L., and C. L. Greengrove, Abyssal eddy in the southwest Atlantic, *Deep-Sea Res., Part A*, 33, 839–847, 1986.
- Groupe CITHER-2 (Le), Recueil de données, campagne CITHER-2, R/V *Maurice Ewing* (4 janvier-21 mars 1994), Volume 2: CTD-O<sub>2</sub>, *Rap. Interne LPO 95-04*, 520 pp., Lab. de Phys. des Océans, Brest, France, 1995.
- Heywood, K. J., and D. P. Stevens, ALBATROSS cruise report, *UEA Cruise Rep. Ser. 6*, Univ. of East Anglia, Norwich, England, U.K., 2000.
- Hogg, N., P. Biscaye, W. Gardener, and W. J. Schmitz, Jr., On the transport and modification of Antarctic Bottom Water in the Vema Channel, *J. Mar. Res.*, 40, suppl., 231–263, 1982.
- Hogg, N. G., G. Siedler, and W. Zenk, Circulation and variability at the southern boundary of the Brazil Basin, *J. Phys. Oceanogr.*, 29, 145–157, 1999.
- Houry, S., E. Dombrowsky, P. De Mey, and J. F. Minster, Brunt-Väisälä frequency and Rossby radii in the South Atlantic, *J. Phys. Oceanogr.*, 17, 1619–1626, 1987.
- Legeckis, R., and A. L. Gordon, Satellite observations of the Brazil and Falkland currents—1975 to 1976 and 1978, *Deep Sea Res., Part A*, 29, 375–401, 1982.
- Maamaatuaiahutapu, K., V. C. Garçon, C. Provost, M. Boulahlid, and A. P. Osiroff, Brazil-Malvinas confluence: Water mass composition, *J. Geophys. Res.*, 97, 9493–9505, 1992.
- Mémery, L., M. Arhan, X. A. Alvarez-Salgado, M.-J. Messias, H. Mercier, C.G. Castro, and A.F. Rios, The water masses along the western boundary of the south and equatorial Atlantic, *Prog. Oceanogr.*, 47, 69–98, 2000.
- Nof, D., Lenses generated by intermittent currents, *Deep Sea Res., Part A*, 38, 325–345, 1991.
- Peterson, R. G., The boundary currents in the western Argentine Basin, *Deep Sea Res., Part A*, 39, 623–644, 1992.
- Peterson, R. G., and T. Whitworth III, The Subantarctic and Polar Fronts in relation to deep water masses through the southwestern Atlantic, *J. Geophys. Res.*, 94, 10,817–10,838, 1989.
- Polvani, L., Two-layer geostrophic dynamics, Part 2, Alignment and two-layer V-states, *J. Fluid Mech.*, 225, 241–270, 1991.
- Quiniou, V., Etude du mécanisme d'instabilité du Courant des Malouines, Rapport de Diplôme d'Etude Approfondies d'Océanogr. Phys., 37 pp., Univ. de Bretagne Occidentale, Brest, France, 2000.
- Reid, J. L., On the total geostrophic circulation of the South Atlantic Ocean: Flow patterns, tracers, and transports, *Prog. Oceanogr.*, 23, 149–244, 1989.
- Reid, J. L., W. D. Nowlin, and W. C. Patzert, On the characteristics and circulation of the southwestern Atlantic Ocean, *J. Phys. Oceanogr.*, 7, 62–91, 1977.
- Schmitt, R. W., Form of the temperature-salinity relationship in the Central Water: Evidence for double-diffusive mixing, *J. Phys. Oceanogr.*, 11, 1015–1026, 1981.
- Scripps Institution Of Oceanography (SIO), Chemical, physical and CTD data reports, Leg 4, 7 December 1988–15 January 1989; Leg 5, 23 January 1989–8 March 1989; R/V *Melville*, SAVE data report, *SIO Ref. 92-10*, 729 pp., Oceanogr. Data Facil., Univ. of Calif., San Diego, 1992.
- Speer, K., and W. Zenk, The flow of Antarctic Bottom water into the Brazil basin, *J. Phys. Oceanogr.*, 23, 2667–2682, 1993.
- Tarbell S., R. Meyer, N. Hogg, and W. Zenk, A moored array along the southern boundary of the Brazil Basin for the Deep Basin Experiment—Report on a joint experiment 1991–1992, *Woods Hole Inst. Tech. Rep. 94-07*, Woods Hole Inst., Woods Hole, Mass., 1994.
- Tychensky, A., and X. Carton, Hydrological and dynamical characterization of meddies in the Azores region: A paradigm for baroclinic vortex dynamics, *J. Geophys. Res.*, 103, 25,061–25,079, 1998.
- Vandermeersch, F., X. Carton, and Y. Morel, The interaction of a vortex with a stable jet, in *Simulation and Identification of Coherent Structures in Flows*, pp. 201–210, Kluwer Acad., Norwell, Mass., 1998.
- Vivier, F., and C. Provost, Volume transport of the Malvinas Current: Can the flow be monitored by TOPEX/POSEIDON?, *J. Geophys. Res.*, 104, 21,105–21,122, 1999.
- Warren, B. A., Divergence of isobaths as a cause of current branching, *Deep Sea Res. Oceanogr. Abstr.*, 16, suppl., 339–355, 1969.
- Weatherly, G. L., On deep-current and hydrographic observations from a mud-wave region and elsewhere in the Argentine Basin, *Deep Sea Res., Part II*, 40, 939–961, 1993.
- Weatherly, G. L., R. H. Evans, and O. T. Brown, A comparison of Geosat altimeter inferred currents and measured flow at 5400 m depth in the Argentine Basin, *Deep Sea Res., Part II*, 40, 989–999, 1993.
- Zenk, W., K. G. Speer, and N. Hogg, Bathymetry at the Vema Sill, *Deep Sea Res., Part I*, 40, 1925–1933, 1993.

M. Arhan and X. Carton, Laboratoire de Physique des Océans, CNRS/IFREMER/UBO, IFREMER/Brest, B.P. 70, 29280 Plouzané, France. (marhan@ifremer.fr)

A. Piola, Servicio de Hidrografia Naval, Montes de Oca 2124, 1271 Buenos Aires, Argentina.

W. Zenk, Institut für Meereskunde, Düsternbrooker Weg 20, 24105 Kiel, Germany.